Received: 19 March 2021 | Revised: 8 September 2021 | Accepted: 14 September 2021
DOI: 10.1111/ppl.13564

ECOPHYSIOLOGY, STRESS AND ADAPTATION

Physiologia Plantarum

# Leaf photosynthetic plasticity does not predict biomass responses to growth irradiance in rice

**Lin Chen** | **Wanzhen Luo** | **Jianliang Huang** | **Shaobing Peng** | **Dongliang Xiong**

National Key Laboratory of Crop Genetic Improvement, Hubei Hongshan Laboratory, MOA Key Laboratory of Crop Ecophysiology and Farming System in the Middle Reaches of the Yangtze River, Huazhong Agricultural University, Wuhan, Hubei, China

**Correspondence**
Dongliang Xiong, National Key Laboratory of Crop Genetic Improvement, Hubei Hongshan Laboratory, MOA Key Laboratory of Crop Ecophysiology and Farming System in the Middle Reaches of the Yangtze River, Huazhong Agricultural University, Wuhan, Hubei 430070, China.
Email: dlxiong@mail.hzau.edu.cn

**Funding information**
National College Students' Innovation and Entrepreneurship Training Programs, Grant/Award Number: HZAU20-01; National Key Research and Development Program of China, Grant/Award Number: 2016YFD0300210

**Edited by** J. Flexas

## Abstract

Phenotypic plasticity, the capacity of an organism to generate alternative phenotypes in response to different environments, is a particularly important characteristic to enable sessile plants to adapt to rapid changes in their surroundings. Leaf anatomical and physiological traits exhibit plasticity in response to growth irradiances, but it is relatively unclear if the plasticity varies among genotypes for a species. Equally importantly, empirical results on how leaf-level plasticity influences whole-plant growth are largely absent. We conducted an integrated investigation into the light-introduced plasticity by measuring 48 traits involving plant growth, leaf anatomy, leaf biochemistry, and leaf physiology of five rice genotypes grown under two irradiances. More than half of the estimated traits were significantly affected by growth light intensities, and the sizes of the cumulative effect of growth light ranged from −25.04% (stomatal conductance at high measurement light) to 135.2% (tiller number). Growth irradiance levels dramatically shifted the relationship between photosynthetic rate and stomatal conductance. However, the relationship between photosynthetic rate and mesophyll conductance was rarely influenced by growth light levels. Importantly, the present study highlights the significant variation in trait plasticity across rice genotypes and that the light-introduced biomass changes were rarely predicted by leaf photosynthetic plasticity. Our findings imply that the genotypes with high productivity at the low growth light conditions do not necessarily have high productivity under high light conditions.

## 1 | INTRODUCTION

Plants capture light to reduce $CO_2$ through photosynthesis, which supports plant growth and supplies the energy for the whole food web. Beyond photosynthesis, light, as a signal, is involved in many aspects of plant development (reviewed by Pham et al., 2018). Due to such an important role of light, the effects of light, mainly intensity, have been widely studied over the past decades and much knowledge has been accumulated in the field. For instance, the short-time responses of photosynthesis of many species are widely evaluated by performing light response curve measurements (Evans et al., 1993). However, the long-term light responses are more complex as most plant traits are shaped by growth light (see the meta-analysis performed by Poorter et al., 2019). Phenotypic changes introduced by light are generally referred to as "plasticity" (Niinemets et al., 2015). Most of the studies in the field focused on the light plasticity of leaves as the predominant organ intercepting light (Niinemets et al., 2015; Poorter et al., 2019).

Growing in the exposed conditions, sun leaves tend to maximize their photosynthetic capacity by increasing leaf thickness to increase nitrogen content on an area basis and the volume of photosynthetic tissues per unit leaf area (Dörken & Lepetit, 2018; Evans & Poorter, 2001; Parkhurst & Loucks, 1972). To prevent overheating due to excessive light capture, sun leaves decline leaf size to enhance

---

Lin Chen and Wanzhen Luo authors contributed equally to this work.

convective heat loss, and increase stomatal density per leaf area to increase transpiration loss rate. In contrast, shade leaves tend to increase specific leaf area (SLA) to capture more light as light is the major limiting resource (Campany et al., 2016; Carins Murphy et al., 2012; Evans & Poorter, 2001). Previous studies suggested that sun- and shade-leaves also differ distinctly in many functional traits along with these anatomical features. To enhance light capture, shade leaves invest more N in the light-harvesting complex, which is reflected by a high chlorophyll to leaf N ratio (Campany et al., 2016; Hikosaka & Terashima, 1995; Xiong, Chen et al., 2015). In sun-exposed leaves, the light-saturated photosynthetic rate, the light compensation point (LCP), the light-saturation irradiance, and leaf hydraulic conductance are significantly higher than in shade leaves (Campany et al., 2016; Dörken & Lepetit, 2018; Niinemets et al., 2015; Poorter et al., 2019; Rozendaal et al., 2006; Scoffoni et al., 2015; Seemann, 1989). Furthermore, the light-induced plasticity in many leaf traits differs significantly among species with different growth habits (Murchie & Horton, 1997; Scoffoni et al., 2015), while the variation of the plasticity degree among genotypes for a given species was rarely studied (Stewart et al., 2017).

Although the light-induced plasticity in leaf anatomy and physiology have been investigated in many previous studies, most of these studies focused on native species, especially woody species, and cereals crops were mostly neglected (even annual grasses; see the studied species the last 90 years summarized by Poorter et al. (2019)). Rice (*Oryza sativa*) is one of the most widely consumed staple foods in the world and is also a widely used model grass species for plant biology (Izawa & Shimamoto, 1996). Revealing the responses of the rice plants to growth irradiance can be crucial. Nowadays, biotechnological-based performance selections, such as high yield and tolerance to stresses, are typically conducted in greenhouses or growth chambers (summarized by Altman et al., 2021). The photosynthetic photo flux density (PPFD) on canopy level is then typically lower than 500 μmol $m^2$ $s^{-1}$, which is very low comparing to the open field condition (e.g. the speed breeding technology, Ghosh et al., 2018). Hence, revealing the light-introduced plasticity in rice plants, especially the genetic variation of plasticity, may help these research designs. Second, the rice canopies, which can be largely influenced by plant density, are typically crowded, and great light gradients commonly appear within the canopy (see Song et al., 2017 and refs therein). Therefore, the canopy photosynthetic capacity might be further improved by considering the light-induced plasticity. Third, the decline in global direct-irradiance, known as global dimming, has been widely observed (Wild et al., 2005), especially in developing regions like Asia, where most rice is grown. Indeed, the impacts of global dimming on rice production have become one of the main current threats in Asia (Shao et al., 2020; e.g. Wang et al., 2015). Understanding light-driven trait plasticity could therefore be important for rice production under future global dimming conditions.

We thus applied an integrated approach to examining plasticity in rice plant growth, physiological, anatomical, and biochemical traits under different growth light intensities. The objectives of the study were (1) to reveal the variations of light-introduced trait plasticity among rice genotypes and (2) to investigate if the differences in biomass accumulation could be explained by the differences in leaf traits, especially the photosynthetic traits.

## 2 | MATERIALS AND METHODS

### 2.1 | Plant materials and treatments

Five rice genotypes, APO, Huanghuazhan (HHZ), IR8, Shanyou 63 (SY63), Yangdao 6 (YD6), were used in this study. These genotypes are widely used in rice biology and/or agronomy studies. Details about the studied genotypes are summarized in Table 1. Three weeks old seedlings were transplanted into 11.0 L pots containing 10 kg dry soil, with a plant density of three plants per pot. For each genotype, 12 pots were prepared. The experiment was conducted on the campus of Huazhong Agricultural University, Wuhan, Hubei, China. The visible water layer in pots was maintained over the experiment period by watering daily. Standard rice practices in fertilizer, herbicide, pesticide, and germicide were adopted to avoid any stress (Wang, Du et al., 2018).

A structure with its top and sides covered by shade cloths was constructed to provide the shading treatment (shade) for half of the plants. The other half of the plants left uncovered in the 100% daylight treatment were considered control (sun). To minimize the air temperature and humidity gradients in and outside the structure, only the east and west sides of the frame were covered but left half of the north and south sides open. The PPFD of the shade treatment was about 30% of the full sun treatment at midday. To minimize the edge effects, pots were randomly rearranged weekly. A typical daily dynamic of light intensity, air temperature and air humidity on the canopies of both sun and shade treatments is shown in Figure S1 and the climate conditions over the experiment are in Table S1. As rice physiological functions are dramatically influenced by sink size at the reproduction and grain filling stages, the measurements/samplings were performed on plants between 60 and 67 days after sowing, when the plants were still at the vegetative stage.

**TABLE 1** Rice genotypes investigated in the current study

| Genotype | Abbreviation | Description |
|---|---|---|
| APO | APO | Upland rice; Known for its tolerance to drought |
| Huanghuazhan | HHZ | A famous “green super rice” in China |
| IR8 | IR8 | Sparked the “green revolution” of rice |
| Shanyou 63 | SY63 | A mega rice hybrid |
| Yangdao 6 | YD6 | A parent of many super rice cultivars released in past decades in China |

## 2.2 | Gas exchange

Gas exchange measurement started on the 60th day after sowing using an LI-6400 (Li-COR Inc.). To minimize the environmental gradients between outside and inside the cuvette of the gas exchange system, the $CO_2$ concentration, relative humidity, and leaf temperature inside the cuvette were set to 400 $\mu$mol mol$^{-1}$, 65%, and 28°C, respectively. Gas exchange measurements were finished in 4 days, and the ambient climate conditions are shown in Table S2. Light response (AQ) curve of photosynthesis was measured through decreasing PPFD from the maximum value of 2000 $\mu$mol m$^{-2}$ s$^{-1}$ to the minimum value of 0 $\mu$mol m$^{-2}$ s$^{-1}$. As the plants were grown under two different light environments, instantaneous point gas exchange measurements were measured at two PPFD levels: 1500 and 500 $\mu$mol m$^{-2}$ s$^{-1}$. The selection of PPFD levels was based on the peak of ambient PPFD on the canopy of sun and shade treatments, respectively (Figure S1). The red to blue ratio was set to 9:1. The newly fully expanded leaves were held in the cuvette (6400-40, Li-COR Inc.) until the photosynthesis values were stable (changes in photosynthetic rate were less than 0.5% over 1 min), which generally occurred rapidly (~3 min), and then the gas exchange parameters and steady-state fluorescence ($F_s$) and maximum fluorescence ($F'_m$) were recorded. Typically, a single measurement was finished in 200 s after the leaf was enclosed in the cuvette. For each treatment, at least six individuals were measured. The actual photochemical efficiency of photosystem II ($\Phi_{PSII}$) was calculated as follows:

$$\Phi_{\mathrm{PSII}} = \frac{\left(F'_{\mathrm{m}} - F_s\right)}{F'_{\mathrm{m}}}$$

The electron transport rate ($J$) was then calculated as follows:

$$J = \Phi_{\mathrm{PSII}} \cdot \mathrm{PPFD} \cdot \alpha\beta$$

Where $\alpha$ is the leaf absorptance and $\beta$ is the partitioning of absorbed quanta between photosystems II and I. The $\alpha\beta$ values were estimated as the slopes of the relationship between $\Phi_{PSII}$ and $4\Phi_{CO2}$ (the quantum efficiency of $CO_2$ uptake) by performing the AQ curves under low $O_2$ conditions (see above and Wang, Du et al., 2018). The variable $J$ method (Harley et al., 1992) was used to calculate the mesophyll conductance ($g_m$):

$$g_{\mathrm{m}} = \frac{A}{\mathrm{C_i} - \frac{\Gamma * (J + 8(A + R_{\mathrm{d}}))}{J - 4(A + R_{\mathrm{d}})}}$$

Where $A$ is the photosynthetic rate, $C_i$ is the $CO_2$ mole fraction in the intercellular air space, $\Gamma^*$ represents the $CO_2$ compensation point in the absence of mitochondrial respiration and $R_d$ is the daytime respiration rate. Typical values of 40 $\mu$mol mol$^{-1}$ and 1 $\mu$mol m$^{-2}$ s$^{-1}$ were used for $\Gamma^*$ and $R_d$, respectively, as they are pretty constant in rice (Wang, Wang et al., 2018; Xiong et al., 2017; Xiong, Liu, et al., 2015). For each $g_m$ generated, we checked whether it met the criterion (10 > $dC_c/dA$ > 50) as recommended by Harley et al. (1992). The "one-point" method (de Kauwe et al., 2016) was used to calculate carboxylation capacity ($V_{cmax}$):

$$V_{\mathrm{cmax}} = A_{1500} \cdot \left(\frac{C_{\mathrm{i}} + K_{\mathrm{m}}}{C_{\mathrm{i}} - K_{\mathrm{m}}} - 0.015\right)$$

where $K_m$ is the apparent Michaelis constant for carboxylation, which was calculated:

$$K_{\mathrm{m}} = k_{\mathrm{c}} \cdot \left(1 + \frac{\mathrm{O_i}}{k_{\mathrm{o}}}\right)$$

where $k_c$ is Michaelis constant for carboxylation, $k_o$ is Michaelis constant for oxygenation, and $O_i$ is oxygen content in the intercellular air space. We chiefly used $k_c$ and $k_o$ values for tobacco from Bernacchi et al. (2001) calibrated to 25°C.

## 2.3 | Leaf optical properties

The leaf color was measured using SPAD 502 (Konica Minolta) after the gas exchange measurement in this study. Eight points were measured in a 5-cm longitudinal distance in the middle of the leaf, and the values were averaged. The leaf thicknesses of both wide and narrow sides were measured using a DTG03 digital thickness gauge (Digital Micrometers Ltd.). For each side of a leaf, 10 points were measured and then the values were averaged.

## 2.4 | Leaf anatomy and elements content

Leaves that performed gas exchange measurements were further used for anatomical and element analysis. Small leaf sections of about 4.0 × 1.2 mm were cut from the top, middle, and bottom of the marked leaves for anatomical analysis. Another part of the sampled leaves was further separated using a leaf tissue punch to measure leaf element content. The leaf pieces were infiltrated with 2.5% glutaric aldehyde (in 0.1 M phosphate buffer; pH = 7.6) fixative solution at 4°C, and post-fixed in 2% buffered osmium tetroxide at 20°C for 2 h. The samples were embedded in Spurr's epoxy resin and cut using a fully automated rotary microtome (Leica RM2265). The leaf sections were stained with 1% (w/v) toluidine blue in 1% (w/v) $Na_2B_4O_7$, and they were examined at 40× and 60× magnification with an Olympus IX71 light microscope. Samples for leaf elements analysis were dried at 70°C to a constant weight and grounded using a mixer mill homogenizer (MM400, Retsch). A subsample of 2.5 mg was used to measure N and C concentration with an NC analyzer (IsoPrime 100 IRMS, Isoprime Ltd.).

## 2.5 | Chlorophyll and Rubisco content

After gas exchange measurement each day (around 11:00 am), the newly fully expanded leaves of the neighbor tillers were sampled for chlorophyll and Rubisco content estimation. About 10-cm leaf blades (leaf areas were fast scanned) at the middle of leaves were sampled. Samples for Rubisco and chlorophyll concentration estimation were quick-frozen using liquid N and stored at −80°C until they were measured. The sample was ground in liquid N (the mortar put on ice), and the ground sample was transferred into a flask using 5 ml of acetone. The mixture was shaken in darkness and then centrifuged at 3000*g* for 20 min, and 1 ml supernatant was collected and dissolved in 5 ml acetone. The solution was further filtered through a 0.22-μm membrane filter and 20 μl of filtered solution was injected for HPLC analysis (LCMS-8050, Shimadzu Corporation). Both chlorophyll *a* and chlorophyll *b* concentrations were measured. The pure standard pigments obtained from Sigma Chemical were used to calibrate the pigment concentrations. For Rubisco estimation, the frozen leaf sample was ground in liquid nitrogen and homogenized in ice in an extraction buffer containing 50 mM Tris-HCl buffer (pH 8.0), 5 mmol β-mercaptoethanol, and 12.5% glycerol (v/v). After centrifuging, the supernatant fluid was extracted for a Rubisco content analysis. The Rubisco samples were loaded onto SDS-PAGE containing a 12.5% (w/v) polyacrylamide gel. After electrophoresis, the gels were washed with deionized water several times, and then dyed in 0.25% Coomassie blue staining solution for 3 h. After that, the gels were decolorized until the background was colorless. The Rubisco bands were transferred into 5-ml cuvettes with 1.5 ml formamide and washed in a 50°C water bath for 8 h and the absorbance (at 595 nm; Infinite M200 Pro, Tecan U.S., Inc) of the solution was measured (Xiong, Liu, et al., 2015).

### 2.6 | Plant growth analysis

The biomass of the whole plant and the main tillers was estimated 70 days after planting. The aboveground part of plants and main tillers were separated into leaf and stem. After leaf area measure using a leaf area meter (Li-3100, Li-COR Inc.), samples were dried at 70°C in an oven, and then the dry weight was determined.

### 2.7 | Data analysis

The effect size and associated variances were calculated to quantify the effects of growth-irradiance levels on plant traits. For a given trait, the effect size (lnR) and the variance ($\upsilon$) for each genotype was calculated as $\ln R = \ln(X_{\text{sun}}/X_{\text{shade}})$ and $\upsilon = \frac{\text{sd}_{\text{sun}}^2}{N_{\text{sun}} \cdot X_{\text{sun}}^2} + \frac{\text{sd}_{\text{shade}}^2}{N_{\text{shade}} \cdot X_{\text{shade}}^2}$, where the X, sd, and *N* are the mean, standard deviations, and sample size of shade or sun treatments, respectively. As the sample size in some cases was not equal, it is not easy to summarize the effect size by using the average lnR for each trait. Alternatively, the cumulative effect size (lnRR) and its confidence interval (CI) of the given trait was calculated as follows:

$$\ln RR = \frac{\sum_{i=1}^{n} \frac{1}{\upsilon_i} (\ln R)_i}{\sum_{i=1}^{n} \frac{1}{\upsilon_i}}$$

where *n* is the number of genotypes (five in the current study), and $(\ln R)_i$ is the effect size for the *i*th genotype. The cumulative effect size represents the overall magnitude of effect (more details about the method see Hedges et al., 1999; Nakagawa & Cuthill, 2007).

Light response curve parameters, including the maximum net photosynthetic rate ($A_{\text{sat}}$), LCP, and PPFD at the 75% saturation photosynthetic rate (LSP), were fitted using the nonrectangular hyperbola-based model (Lobo et al. 2013):

$$A = \frac{\Phi \times \text{PPFD} + A_{\text{gmax}} - \sqrt{(\Phi \times \text{PPFD} + A_{\text{gmax}})^2 - 4\theta \times \Phi \times \text{PPFD} \times A_{\text{gmax}}}}{2\theta} - R_{\text{n}}$$

where $\Phi$ is the quantum yield at PPFD = 0 μmol (photon) $\text{m}^{-2}$ $\text{s}^{-1}$, $A_{\text{gmax}}$ is the maximum gross photosynthetic rate, $\theta$ is the convexity factor, and $R_{\text{n}}$ is dark respiration. The model was fitted to the data using the Orthogonal Nonlinear Least-Squares Regression (*onls*) function. Parametric ANOVA, principal component analysis (PCA), and standardized major axis estimation were performed using packages of *agricolae*, *FactoMineR*, *and smatr*, respectively. Other analyses and plots were conducted using the *tidyverse* package. All analyses were performed in R 3.6.3 platform (R Core Team, 2020).

## 3 | RESULTS

### 3.1 | Effects of light intensities on rice growth

All growth traits varied significantly across genotypes, except for leaf mass per plant (ANOVA, Table 2). By averaging trait values for each genotype across two irradiance levels, a substantial variation in growth traits among the five genotypes was observed, except for leaf mass per plant (ANOVA, Table 2). All the growth traits were significantly affected by the shading treatment (Table 2; Figure 1). Biomass, tiller number per plant, and leaf area values were substantially higher for plants grown at high irradiance conditions than those for plants grown at low irradiance conditions (Table S3). Overall, the cumulative effect of growth irradiance ranged from −21.44% (LTBR) to 135.2% (TN). Seven of eleven growth traits showed positive responses to light in all the genotypes, and four traits showed negative responses to light (Figure 2). The tiller number increased by 135% under high irradiance conditions from the low light conditions, and the biomass of the plant increased by 85.0% (Figure 2). Interestingly, the increase of biomass per plant under high irradiance conditions was mainly caused by the increase of stem biomass (increased by 114.0%). However, the light-introduced plasticity of growth traits was genotype-dependent. For instance, HHZ declined leaf area and leaf mass per plant at shade condition, which showed a contrary response referring to the other four genotypes (Table S3).

### 3.2 | Effects of light intensities on leaf anatomy

Among the rice genotypes, a substantial variation in LMA, leaf thickness, venation density, epidermis proportion, and bulliform proportion

**TABLE 2** The results of the ANOVA testing the traits effects of genotype (*G*), growth irradiance (*I*), and their interaction ($G \times I$)

| Trait | Symbol | Unit | G | I | G × I |
|---|---|---|---|---|---|
| *1. Plant growth* | | | | | |
| Biomass | BM | g plant$^{-1}$ | * | *** | * |
| Tiller number | TN | plant$^{-1}$ | *** | *** | ** |
| Plant height | PH | cm | *** | *** | ** |
| Leaf Area per plant | LAPP | cm$^{2}$ | * | *** | ns |
| Stem mass per plant | SMPP | g | * | *** | ns |
| Leaf mass per plant | LMPP | g | ns | *** | ns |
| Leaf mass to biomass mass ratio | LTBR | g g$^{-1}$ | *** | *** | ns |
| Biomass per tiller | BMPT | g tiller$^{-1}$ | *** | ** | ns |
| Leaf area per tiller | LAPT | cm$^{2}$ tiller$^{-1}$ | ** | * | ns |
| Stem mass per tiller | STPT | g tiller$^{-1}$ | *** | *** | ns |
| Leaf mass per tiller | LMPT | g tiller$^{-1}$ | *** | ** | ** |
| *2. Leaf anatomy* | | | | | |
| Leaf mass per area | LMA | g m$^{-2}$ | *** | ** | * |
| Leaf thickness-wide side | $LT_W$ | mm | ** | ns | ns |
| Leaf thickness-narrow side | $LT_N$ | mm | ns | ns | ns |
| Major vein density | $VLA_{major}$ | mm mm$^{-2}$ | * | * | ns |
| Minor vein density | $VLA_{minor}$ | mm mm$^{-2}$ | ** | *** | ns |
| Total vein density | VLA | mm mm$^{-2}$ | ** | *** | ns |
| Major vein thickness | $LT_{major}$ | μm | ns | ns | ns |
| Minor vein thickness | $LT_{minor}$ | μm | ns | * | *** |
| Mesophyll tissue proportion | $f_{mesophyll}$ | % | ns | ns | ns |
| Major vein tissue proportion | $f_{majorvein}$ | % | ns | ns | ns |
| Minor vein tissue proportion | $f_{minorvein}$ | % | ** | ns | * |
| Upper epidermis proportion | $f_{up\text{-}epidermises}$ | % | ** | ns | ns |
| Lower epidermis proportion | $f_{low\text{-}epidermises}$ | % | *** | ns | ns |
| Bulliform proportion | $f_{bulliform}$ | % | *** | ns | ns |
| *3. Leaf biochemistry* | | | | | |
| SPAD value | SPAD | unitless | *** | ns | ** |
| Leaf N content | $N_{area}$ | g m$^{-2}$ | *** | * | *** |
| Leaf N concentration | $N_{mass}$ | % | *** | ns | ns |
| Leaf C content | $C_{area}$ | g m$^{-2}$ | *** | *** | *** |
| Carbon concentration | $C_{mass}$ | % | * | ns | * |
| Carbon to nitrogen ratio | CTNR | – | *** | ns | ns |
| Chlorophyll *a* content | Chla | μmol m$^{-2}$ | *** | *** | ** |
| Chlorophyll *b* content | Chlb | μmol m$^{-2}$ | *** | *** | ** |
| Total chlorophyll content | Chl(a + b) | μmol m$^{-2}$ | *** | *** | ** |
| Molar Chl *a* to *b* ratio | Chla/b | – | *** | *** | ns |
| Rubisco content | Rubisco | g m$^{-2}$ | *** | ns | ns |
| *4. leaf physiology* | | | | | |
| Photosynthesis at high light | $A_{1500}$ | μmol m$^{-2}$ s$^{-1}$ | *** | ns | ns |
| Photosynthesis at low light | $A_{500}$ | μmol m$^{-2}$ s$^{-1}$ | ns | ns | ns |
| Stomatal conductance at high light | $g_{sw\_1500}$ | mol m$^{-2}$ s$^{-1}$ | * | ** | *** |
| Stomatal conductance at low light | $g_{sw\_500}$ | mol m$^{-2}$ s$^{-1}$ | ns | * | ns |
| Water use efficiency at high light | $WUE_{1500}$ | μmol mol$^{-1}$ | ns | * | ns |
| Water use efficiency at low light | $WUE_{500}$ | μmol mol$^{-1}$ | ns | * | ns |

(Continues)

**TABLE 2** (Continued)

| Trait | Symbol | Unit | G | *I* | G × *I* |
|---|---|---|---|---|---|
| Mesophyll conductance at high light | $g_{m\_1500}$ | mol m$^{-2}$ s$^{-1}$ | ns | ns | ns |
| Mesophyll conductance at low light | $g_{m\_500}$ | mol m$^{-2}$ s$^{-1}$ | ns | ns | ns |
| Carboxylation capacity | $V_{cmax}$ | μmol m$^{-2}$ s$^{-1}$ | ns | * | ns |
| Light saturated photosynthesis | $A_{sat}$ | μmol m$^{-2}$ s$^{-1}$ | ns | ns | *** |
| Light compensation point | LCP | μmol m$^{-2}$ s$^{-1}$ | ns | ns | *** |

*Note*: ns, $p > 0.05$.
*, $p < 0.05$.
**, $p < 0.01$.
***, $p < 0.001$.

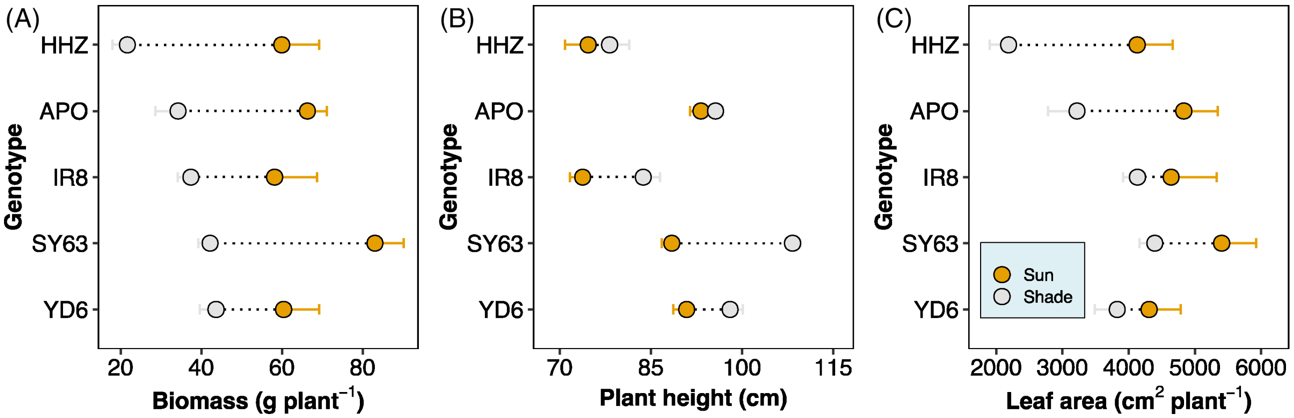

**FIGURE 1** Plastic response of plant growth traits in response to growth irradiance for five rice genotypes. Aboveground biomass (A), plant height (B), and total leaf area per plant (C). Bars represent standard errors, and the black dots lines represent the average differences between irradiance treatments. Traits were estimated 70 days after sowing. N = 10 individual plants

were found (Table 2). Across the two growth irradiance conditions, the LMA varied from 37.4 to 50.4 g m$^{-2}$ and VLA from 4.02 to 5.72 mm mm$^2$. Unexpectedly, nine of fourteen leaf anatomical traits showed no response to growth irradiance according to the ANOVA outputs (Table 2). Thus, the absolute values of the accumulative effect size of leaf anatomical traits were relatively small (Figure 2). LMA and venation traits showed significant plasticity to growth irradiance. Indeed, the increase of LMA and venation traits at high irradiance conditions were greater than other anatomical traits (Figure 2). By contrast, the proportion of upper epidermis cells and bulliform cells declined at high irradiance conditions. Notably, the responses of leaf anatomical traits to growth irradiance were genotype-dependent, and some of the genotypes showed contrary responses (Table S4).

## 3.3 | Effects of light intensities on leaf biochemical traits

Significant variations in all 11 leaf biochemical traits across the five rice genotypes were found (ANOVA; Table 2; Table S5). Overall, leaf biochemical traits were significantly shifted by growth irradiance, except for SPAD values, $N_{mass}$ $C_{mass}$, CTNR, and Rubisco content. Rice genotypes differed in the plasticity of most of the biochemical traits measured, including SPAD, $N_{area}$, $C_{mass}$, $C_{area}$, and chlorophyll content (ANOVA analysis for genotype and growth light interaction; Table 2). For leaves developed under high light conditions, the chlorophyll *a* and *b* content declined, but area-based C and N content and Rubisco content increased (Figure 2). However, the decrease of chlorophyll *b* was more remarkable than chlorophyll *a* under high irradiance conditions, and thus the chlorophyll *a* to *b* ratio increased.

## 3.4 | Effects of light intensities on leaf function

On average, no significant difference was observed for gas exchange traits among rice genotypes, except for $A_{1500}$, $g_{sw\_1500}$, and LSP (ANOVA; Table 2). Gas exchange traits were less influenced by growth irradiance, except for stomatal conductance, water use efficiency, and $V_{cmax}$. Surprisingly, no differences were observed in light-saturated photosynthetic rate ($A_{sat}$, fitted from light response curves; Figure S3) between two growth irradiances. No significant difference was observed in the net photosynthetic rate of sun and shade leaves (Table 2; Figures 2 and 3). The mean (across genotypes) value of stomatal conductance of shade leaves was higher than that of sun leaves at two measured light levels (Figure S4).

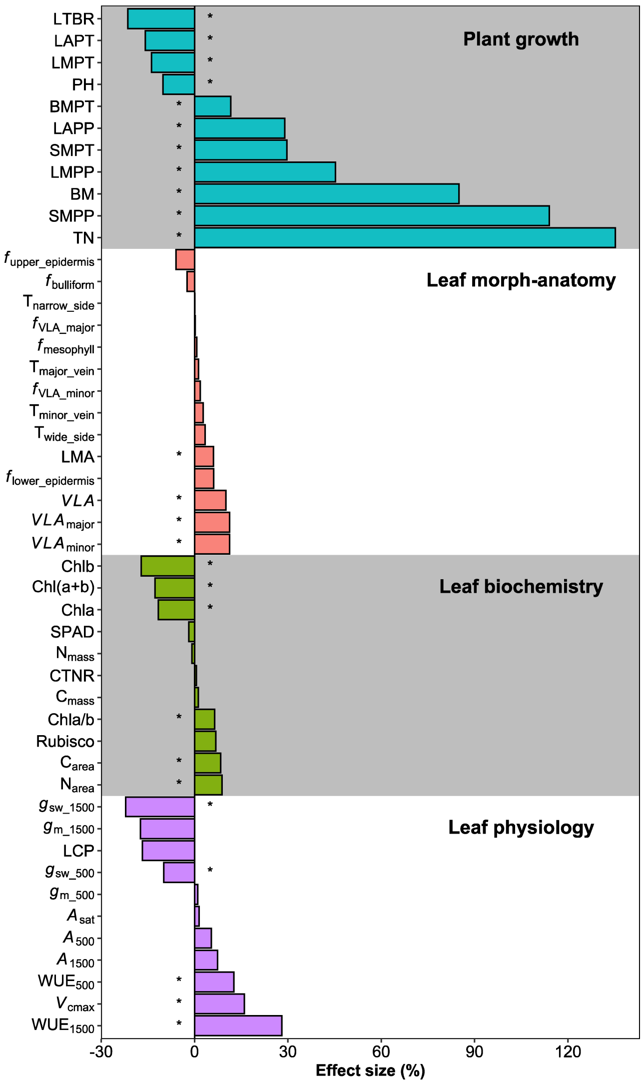

**FIGURE 2** The accumulative effect size of estimated traits. Horizontal bars denote the effect size (calculations see M&M section) and the asterisk represents a significant effect (confidence intervals did not cover 0) for the trait. A positive, zero, and negative effect size correspond to a higher, equal, and lower value under sun conditions than under shade conditions, respectively. See Table 2 for definitions of the variables. N = 5–10 individual plants

In contrast, no differences in mesophyll conductance between sun and shade leaves were observed when measured at the low light condition; however, the mesophyll conductance of sun leaves was higher than that of shade leaves when measured at the high light conditions. Unlike the stomatal conductance, the mesophyll conductance showed a strong response to light intensity. Genotypes varied greatly in the patterns and degrees of their physiological traits' plastic responses. For instance, the stomatal conductances of shade leaves were the doubled of sun leaves for IR8 under both low and high measurement light conditions. However, the stomatal conductances of shade leaves for SY63 and HHZ were lower than that of sun leaves when measured at low and high light conditions, respectively (Figure 4; Table S6).

Although the *A* was positively correlated to $g_{\mathrm{sw}}$, both slopes and intercepts of the regression lines differed significantly under different growth irradiance (standardized major axis analysis; Figure 3). The relationship between *A* and $g_{\mathrm{m}}$ showed an opposite response: the slopes and intercepts of the regression lines showed no differences between low and high growth irradiances, except for the intercepts under high measurement light ($p = 0.03$; Figure 3).

## 3.5 | Multivariate trait (Co)variation

PCA, a multivariate technique, revealed a distinct separation between sun and shade treatments, and the separation was greater along the first principal component axis (PC1; Figure 4). The first PCA axis accounted for 27.1% of the total variation and showed strong loadings on growth traits such as tiller number, leaf and stem biomass, and leaf mass to biomass ratio. The second axis, which accounted for 22.7% of the total variation, had strong loadings on gas exchange traits, proportions of epidermis and mesophyll tissues, and chlorophyll concentrations. The loadings of photosynthetic rates were close to mesophyll and stomatal conductance but almost perpendicular to growth traits, including biomass, tiller number, and leaf mass to biomass ratio.

# 4 | DISCUSSION

## 4.1 | Plastic response of the leaf traits to growth irradiances

Leaves developed under shade conditions (shade leaves) should have higher SLA (the reciprocal of LMA), large leaf area, and lower thickness than leaves grown under sun conditions (reviewed by Poorter et al., 2019 and refs therein). Our LMA and leaf area data agree with the conventional conclusions, although the differences between sun and shade leaves were not significant for some of the genotypes. However, a heterogeneous response of leaf thickness to growth irradiances was observed: a declined leaf thickness on the wide side of the leaf but no changes on the narrow side (Table 2). The mechanisms regulating the asymmetric changes of leaf thickness are still unclear, and future investigations are required. Consistent with a few previous studies, smaller sun leaves had higher VLA resulting from higher major and minor vein density, which may improve the water transport capacity to cool leaves (Carins Murphy et al., 2012; Scoffoni et al., 2015).

The shifts in leaf area and LMA corresponded to the increases of area-based leaf carbon, N content, and Rubisco content under high light conditions. As frequently observed in previous studies, both chlorophyll *a* and *b* increased in shade leaves and the higher increase of chlorophyll *b* resulted in a decreased ratio of chlorophyll *a* to *b* (Dörken & Lepetit, 2018; Poorter et al., 2019). In general, chlorophyll *a* is recognized as an effective pigment for photosynthesis at the blue and red bands and chlorophyll *b* has less efficiency in absorbing blue light (Esteban et al., 2015). Indeed, the light response of the chlorophyll *a* to *b* ratio is well explained by the photosynthetic nitrogen economy. An increase in light-harvesting complex II, which contains

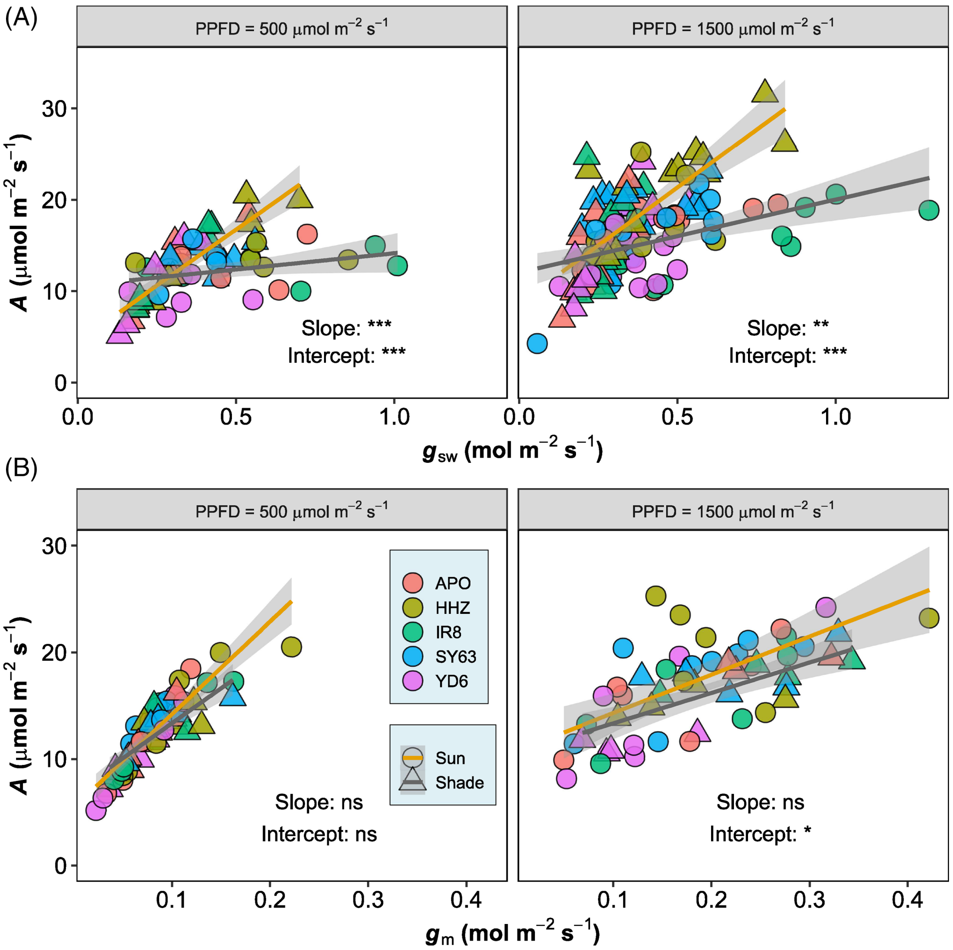

**FIGURE 3** The relationships between leaf photosynthetic rate (*A*), stomatal conductance ($g_s$, Panel A) and mesophyll conductance ($g_m$, panel B) for sun and shade leaves measured with two-sets of PPFD inside Li-COR 6400 chamber. Lines represent smoothed regressions from the linear model fits. Gray area are 95% confidence intervals for the mean. In each panel, the allometry of the lines was estimated using standardized major axis method in the *r* package *smatr*. Asterisks represent the significant levels between treatments estimated using the standardized major axis model. ***, $p < 0.001$; **, $p < 0.01$; *, $p < 0.05$; ns, $p > 0.05$. N = 5–10 individual plants

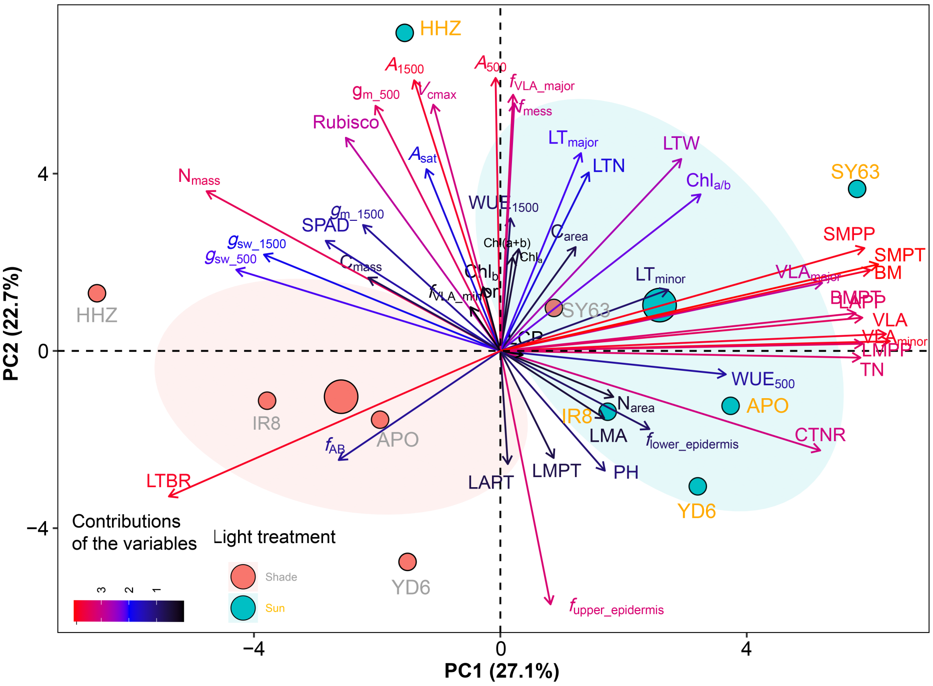

**FIGURE 4** Biplot of principal component analysis (PCA) showing principal component scores of rice individuals (small dots) and loadings of variables (vectors). Ellipses represent 95% confidences of the group means (large dots). PC1 and PC2 represent the first two principal components. See Table 2 for definitions of the variables

more chlorophyll *b* than in PSII core complex, benefits light absorption under low light conditions (Evans & Terashima, 1987).

Leaves developed in high irradiance conditions have higher photosynthetic capacities (i.e. $V_{cmax}$) than leaves developed in low irradiance conditions, resulting from higher Rubisco content. However, the light-saturated photosynthesis ($A_{sat}$, fitted from light response curves) showed no difference between the sun and shade leaves, which supports previous results indicating that rice $A_{sat}$ is related to $V_{cmax}$, and other traits (Xiong & Flexas, 2018). The observation of no difference in net photosynthetic rate between the sun and shade rice leaves (Table 2; Figure 2) disagrees with some previous studies where leaves could acclimate to environmental light intensities (Dörken & Lepetit, 2018; Seemann, 1989; Senevirathna et al., 2003). As $V_{cmax}$ declined in shade leaves, high photosynthetic rates in shade leaves could relate to their high $g_{sw}$.

Photosynthetic rate (*A*) was positively correlated with $g_{sw}$ in sun leaves, which is consistent with the optimal theory (Farquhar & Wong, 1984). However, the slope of the $A$-$g_{sw}$ regression was much lower in shade leaves than in sun leaves, which was also confirmed by the low WUE in shade leaves (Table 2). Considering rice plants typically grow in paddy fields where soil water potential is relatively stable over the growing season, leaving the stomata pore open in shading conditions might be an effective strategy to use sun-fleck. Indeed, an unexpected high $g_{sw}$ in shading leaves has been observed in several woody species (Campany et al., 2016; Scoffoni et al., 2015; Vico et al., 2011). It is worth noting that the growth-irradiance response of $g_{sw}$ varied significantly across genotypes, indicating different stomatal adaption mechanisms might exist. Further work is needed to reveal the mechanisms behind the complex light response behaviors. Unexpectedly, the $g_m$ was not affected by growth irradiance but dramatically influenced by measurement light intensities. Although the leaf structures have been suggested to determine $g_m$ variation across species (Tomás et al., 2013), the structural modifications unlikely corresponded to the short-time light response of $g_m$ in rice. Ignoring the recently raised methodology problems in estimating $g_m$ (Gu & Sun, 2014), possible mechanisms for the short-term light response $g_m$ include regulation of aquaporins and chloroplast movement (reviewed by Flexas et al., 2018).

## 4.2 | Leaves to whole plant responses

Leaf traits, especially photosynthetic traits, are widely used to summarize and predict/model the species response to environmental factors (reviewed by Niinemets et al., 2015; Poorter et al., 2019). Our results highlighted that neither leaf-level *A* plasticity nor $A_{sat}$ plasticity could predict the whole-plant biomass response to growth irradiance. Indeed, the PCA analysis clearly showed that whole-plant traits mainly separated the shade and sun treatments and the photosynthetic rates had very limited contribution in such separation (Figure 4). On single tiller scale, the difference of leaf area between sun and shade treatments was relatively small, and the genotypes with more tillers, for instance, SY63 and YD6, tended to have high biomass accumulations under low irradiance. Whole-plant growth results from net canopy photosynthesis over the growing season, rather than the *A* or $A_{sat}$ of newly expanded individual leaves. At a given moment, the canopy assimilation rate is the sum of the photosynthetic rate of individual leaves within the canopy. The environmental gradients, including light availability and temperature, are the most striking feature of canopies (Song et al., 2013). Leaves in different canopy positions have different light availability regulated by the geometry and the dynamics of a canopy and thus result in different *A*. Moreover, heterogeneous photosynthetic capacities within the canopy are also expected as the leaves developed at different times and environmental conditions. For instance, at a given environmental condition, the *A* of leaves varied significantly at each ontogenetic stage (Mason et al., 2013). The crop canopy develops dynamically over the growing season, and the biomass accumulation could efficiency relate to different canopy development strategies. Beyond photosynthetic rate, N allocation among organs and tissues was suggested to determine the growth performance (Hikosaka, 2014; Makino et al., 1997). In the current study, we found that the C to N ratio (CTNR) and the leaf vein density (VLA) closely relates to tiller scale and plant scale growth performance (Figure 4). Although further work is needed to confirm such relationships, CTNR and VLA might be useful traits for high yield germplasm selection.

## 4.3 | Genetic variation and its implications

Trait plasticity is a major mechanism by which plants cope with dynamic environments and is proposed as informative in predicting how species will respond to changing future climate conditions. Although variation in traits plasticity is known to exist among species, relatively few studies have examined variation within crop species. Here, genotyping variations in trait plasticity (i.e. growth traits) were found in rice. For instance, the growth irradiance effect size of biomass was 102% for HHZ but only 32% for YD6. For the photosynthetic traits, including $A_{1500}$, $g_m$, and $g_{sw}$, the growth irradiance responses were in contrast direction for different genotypes. Although the physiological or genetic mechanisms underlying these differences are still largely unknown, significant intraspecific variation in trait plasticity exists, providing a valuable source of unexploited genetic diversity for rice breeding under future global dimming. The result, however, criticized the greenhouse-based breeding selections, a popular modern breeding approach (summarized in Ghosh et al., 2018), because the genotypes with good performance at low growth irradiances (e.g. in the greenhouse) do not necessarily have the best performance under high light conditions (e.g. open field) compared with other genotypes.

**ACKNOWLEDGMENTS**

This study was supported by National Key Research and Development Program of China (2016YFD0300210). Lin Chen and Wanzhen Luo were supported by the National College Students' Innovation and Entrepreneurship Training Programs (HZAU20-01). Lin Chen and Wanzhen Luo would gratefully acknowledge the skillful technical assistance of Xiaoxiao Wang, Tingting Du, Xianhong Huang, Zhuang Xiong, and Qiaoyun Zhang and appreciate Mei Feng, Panpan Xiong, and Tao Zhang from the student office for their favor and support.

## CONFLICT OF INTEREST

The authors declare that they have no conflict of interest associated with this work.

## AUTHOR CONTRIBUTIONS

Dongliang Xiong conceived the ideas and designed methodology with the help of Jianliang Huang, Shaobing Peng; Lin Chen and Wanzhen Luo conducted the experiments; Dongliang Xiong analyzed data and wrote the first draft of the paper. All authors contributed critically to the draft and gave final approval for publication.

## DATA AVAILABILITY STATEMENT

All relevant data supporting the results presented in this work are available within the article and the supporting materials.

## ORCID

*Jianliang Huang* https://orcid.org/0000-0002-4700-0329
*Dongliang Xiong* https://orcid.org/0000-0002-6332-2627

## REFERENCES

Altman, A., Fan, L., Foyer, C., Cowling, W., Mittler, R., Qaim, M. et al. (2021) Past and future milestones of plant breeding. *Trends in Plant Science*, 26, 530–538.

Bernacchi, C.J., Singsaas, E.L., Pimentel, C., Portis, A.R., Jr. & Long, S.P. (2001) Improved temperature response functions for models of Rubisco-limited photosynthesis. *Plant, Cell & Environment*, 24, 253–259.

Campany, C.E., Tjoelker, M.G., von Caemmerer, S. & Duursma, R.A. (2016) Coupled response of stomatal and mesophyll conductance to light enhances photosynthesis of shade leaves under sunflecks. *Plant, Cell & Environment*, 39, 2762–2773.

Carins Murphy, M.R., Jordan, G.J. & Brodribb, T.J. (2012) Differential leaf expansion can enable hydraulic acclimation to sun and shade. *Plant, Cell & Environment*, 35, 1407–1418.

de Kauwe, M.G., Lin, Y.-S., Wright, I.J., Medlyn, B.E., Crous, K.Y., Ellsworth, D.S. et al. (2016) A test of the 'one-point method' for estimating maximum carboxylation capacity from field-measured, light-saturated photosynthesis. *The New Phytologist*, 210, 1130–1144.

Dörken, V.M. & Lepetit, B. (2018) Morpho-anatomical and physiological differences between sun and shade leaves in *Abies alba* Mill. (Pinaceae, Coniferales): a combined approach. *Plant, Cell & Environment*, 41, 1683–1697.

Esteban, R., Barrutia, O., Artetxe, U., Fernández-Marín, B., Hernández, A. & García-Plazaola, J.I. (2015) Internal and external factors affecting photosynthetic pigment composition in plants: a meta-analytical approach. *The New Phytologist*, 206, 268–280.

Evans, J.R., Jakobsen, I. & Ogren, E. (1993) Photosynthetic light-response curves. *Planta*, 189, 191–200.

Evans, J.R. & Poorter, H. (2001) Photosynthetic acclimation of plants to growth irradiance: the relative importance of specific leaf area and nitrogen partitioning in maximizing carbon gain. *Plant, Cell & Environment*, 24, 755–767.

Evans, J.R. & Terashima, I. (1987) Effects of nitrogen nutrition on electron transport components and photosynthesis in spinach. *Functional Plant Biology*, 14, 59.

Farquhar, G.D. & Wong, S.C. (1984) An empirical model of stomatal conductance. *Functional Plant Biology*, 11, 191.

Flexas, J., Cano, F.J., Carriquí, M., Coopman, R.E., Mizokami, Y., Tholen, D. et al. (2018) $CO_2$ diffusion inside photosynthetic organs. In: Adams, W.W. & Terashima, I. (Eds.) *The leaf. A platform for performing photosynthesis*. Cham: Springer, pp. 163–208.

Ghosh, S., Watson, A., Gonzalez-Navarro, O.E., Ramirez-Gonzalez, R.H., Yanes, L., Mendoza-Suárez, M. et al. (2018) Speed breeding in growth chambers and glasshouses for crop breeding and model plant research. *Nature Protocols*, 13, 2944–2963.

Gu, L. & Sun, Y. (2014) Artefactual responses of mesophyll conductance to $CO_2$ and irradiance estimated with the variable J and online isotope discrimination methods. *Plant, Cell & Environment*, 37, 1231–1249.

Harley, P.C., Loreto, F., Di Marco, G. & Sharkey, T.D. (1992) Theoretical considerations when estimating the mesophyll conductance to $CO_2$ flux by analysis of the response of photosynthesis to $CO_2$. *Plant Physiology*, 98, 1429–1436.

Hedges, L.V., Gurevitch, J. & Curtis, P.S. (1999) The meta-analysis of response ratios in experimental ecology. *Ecology*, 80, 1150–1156.

Hikosaka, K. (2014) Optimal nitrogen distribution within a leaf canopy under direct and diffuse light. *Plant, Cell & Environment*, 37, 2077–2085.

Hikosaka, K. & Terashima, I. (1995) A model of the acclimation of photosynthesis in the leaves of $C_3$ plants to sun and shade with respect to nitrogen use. *Plant, Cell & Environment*, 18, 605–618.

Izawa, T. & Shimamoto, K. (1996) Becoming a model plant: the importance of rice to plant science. *Trends in Plant Science*, 1, 95–99.

Lobo, F.A., Barros, M.P., Dalmagro, H.J., Dalmolin, A.C., Pereira, W.E., Souza, E.C. et al. (2013) Fitting net photosynthetic light-response curves with Microsoft excel - a critical look at the models. *Photosynthetica*, 51, 445–456.

Makino, A., Sato, T., Nakano, H. & Mae, T. (1997) Leaf photosynthesis, plant growth and nitrogen allocation in rice under different irradiances. *Planta*, 203, 390–398.

Mason, C.M., McGaughey, S.E. & Donovan, L.A. (2013) Ontogeny strongly and differentially alters leaf economic and other key traits in three diverse Helianthus species. *Journal of Experimental Botany*, 64, 4089–4099.

Murchie, E.H. & Horton, P. (1997) Acclimation of photosynthesis to irradiance and spectral quality in British plant species: chlorophyll content, photosynthetic capacity and habitat preference. *Plant, Cell & Environment*, 20, 438–448.

Nakagawa, S. & Cuthill, I.C. (2007) Effect size, confidence interval and statistical significance: a practical guide for biologists. *Biological Reviews of the Cambridge Philosophical Society*, 82, 591–605.

Niinemets, Ü., Keenan, T.F. & Hallik, L. (2015) A worldwide analysis of within-canopy variations in leaf structural, chemical and physiological traits across plant functional types. *The New Phytologist*, 205, 973–993.

Parkhurst, D.F. & Loucks, O.L. (1972) Optimal leaf size in relation to environment. *The Journal of Ecology*, 60, 505.

Pham, V.N., Kathare, P.K. & Huq, E. (2018) Phytochromes and Phytochrome interacting factors. *Plant Physiology*, 176, 1025–1038.

Poorter, H., Niinemets, Ü., Ntagkas, N., Siebenkäs, A., Mäenpää, M., Matsubara, S. et al. (2019) A meta-analysis of plant responses to light intensity for 70 traits ranging from molecules to whole plant performance. *The New Phytologist*, 223, 1073–1105.

R Core Team (2020) *R: a language and environment for statistical computing*. Available at: https://www.R-project.org.

Rozendaal, D., Hurtado, V. & Poorter, L. (2006) Plasticity in leaf traits of 38 tropical tree species in response to light; relationships with light demand and adult stature. *Functional Ecology*, 20, 207–216.

Scoffoni, C., Kunkle, J., Pasquet-Kok, J., Vuong, C., Patel, A.J., Montgomery, R.A. et al. (2015) Light-induced plasticity in leaf hydraulics, venation, anatomy, and gas exchange in ecologically diverse Hawaiian lobeliads. *The New Phytologist*, 207, 43–58.

Seemann, J.R. (1989) Light adaptation/acclimation of photosynthesis and the regulation of Ribulose-1,5-Bisphosphate Carboxylase activity in sun and shade plants. *Plant Physiology*, 91, 379–386.

Senevirathna, A.M., Stirling, C.M. & Rodrigo, V.H. (2003) Growth, photosynthetic performance and shade adaptation of rubber (*Hevea brasiliensis*) grown in natural shade. *The New Phytologist*, 23, 705–712.

Shao, L., Liu, Z., Li, H., Zhang, Y., Dong, M., Guo, X. et al. (2020) The impact of global dimming on crop yields is determined by the source-sink imbalance of carbon during grain filling. *Global Change Biology*, 27, 689–708.

Song, Q., Wang, Y., Qu, M., Ort, D.R. & Zhu, X.-G. (2017) The impact of modifying photosystem antenna size on canopy photosynthetic efficiency-development of a new canopy photosynthesis model scaling from metabolism to canopy level processes. *Plant, Cell & Environment*, 40, 2946–2957.

Song, Q., Zhang, G. & Zhu, X.-G. (2013) Optimal crop canopy architecture to maximise canopy photosynthetic $CO_2$ uptake under elevated $CO_2$—a theoretical study using a mechanistic model of canopy photosynthesis. *Functional Plant Biology*, 40, 108–124.

Stewart, J.J., Polutchko, S.K., Adams, W.W. & Demmig-Adams, B. (2017) Acclimation of Swedish and Italian ecotypes of *Arabidopsis thaliana* to light intensity. *Photosynthesis Research*, 134, 215–229.

Tomás, M., Flexas, J., Copolovici, L., Galmés, J., Hallik, L., Medrano, H. et al. (2013) Importance of leaf anatomy in determining mesophyll diffusion conductance to $CO_2$ across species: quantitative limitations and scaling up by models. *Journal of Experimental Botany*, 64, 2269–2281.

Vico, G., Manzoni, S., Palmroth, S. & Katul, G. (2011) Effects of stomatal delays on the economics of leaf gas exchange under intermittent light regimes. *The New Phytologist*, 192, 640–652.

Wang, L., Deng, F. & Ren, W.-J. (2015) Shading tolerance in rice is related to better light harvesting and use efficiency and grain filling rate during grain filling period. *Field Crops Research*, 180, 54–62.

Wang, X., Du, T., Huang, J., Peng, S. & Xiong, D. (2018) Leaf hydraulic vulnerability triggers the decline in stomatal and mesophyll conductance during drought in rice. *Journal of Experimental Botany*, 69, 4033–4045.

Wang, X., Wang, W., Huang, J., Peng, S. & Xiong, D. (2018) Diffusional conductance to $CO_2$ is the key limitation to photosynthesis in salt-stressed leaves of rice (*Oryza sativa*). *Physiologia Plantarum*, 163, 45–58.

Wild, M., Gilgen, H., Roesch, A., Ohmura, A., Long, C.N., Dutton, E.G. et al. (2005) From dimming to brightening: decadal changes in solar radiation at Earth's surface. *Science (New York, N.Y.)*, 308, 847–850.

Xiong, D., Chen, J., Yu, T., Gao, W., Ling, X., Li, Y. et al. (2015) SPAD-based leaf nitrogen estimation is impacted by environmental factors and crop leaf characteristics. *Scientific Reports*, 5, 13389.

Xiong, D. & Flexas, J. (2018) Leaf economics spectrum in rice: leaf anatomical, biochemical, and physiological trait trade-offs. *Journal of Experimental Botany*, 69, 5599–5609.

Xiong, D., Flexas, J., Yu, T., Peng, S. & Huang, J. (2017) Leaf anatomy mediates coordination of leaf hydraulic conductance and mesophyll conductance to $CO_2$ in *Oryza*. *New Phytologist*, 213, 572–583.

Xiong, D., Liu, X., Liu, L., Douthe, C., Li, Y., Peng, S. et al. (2015) Rapid responses of mesophyll conductance to changes of $CO_2$ concentration, temperature and irradiance are affected by N supplements in rice. *Plant, Cell & Environment*, 38, 2541–2550.

## SUPPORTING INFORMATION

Additional supporting information may be found in the online version of the article at the publisher's website.

**How to cite this article:** Chen, L., Luo, W., Huang, J., Peng, S. & Xiong, D. (2021) Leaf photosynthetic plasticity does not predict biomass responses to growth irradiance in rice. *Physiologia Plantarum*, 1–11. Available from: https://doi.org/10.1111/ppl.13564